Catal Lett (2008) 125:104–109
DOI 10.1007/s10562-008-9521-6

S–N Co-Doped TiO_2 Photocatalysts with Visible-Light Activity Prepared by Sol–Gel Method

Xiang Li · Rongchun Xiong · Gang Wei

Received: 20 March 2008 / Accepted: 14 May 2008 / Published online: 4 June 2008

Abstract S–N co-doped anatase nanosized TiO_2 photocatalyst was successfully prepared by simple sol–gel method. The samples were characterized by XRD, XPS, UV–Vis. From the results of UV–Vis, a red shift of the absorption edge was brought out owing to the S and N codoping. XPS and UV–Vis studies revealed that N and S were in situ codoped in the lattice of TiO_2 and the absorbance in visible light region decreased with the calcination temperature increased. The photocatalytic activity was evaluated by the photocatalytic oxidation of penicillin solution under visible light irradiation. The results show that visible-light induced photocatalytic activities of the as-prepared TiO_2 powders were improved by S–N copoing. The high activity of S–N co-doped TiO_2 can be related to the results of the synergetic effects of strong absorption in the UV–Vis region, red shift in adsorption edge.

Keywords S and N codoping · Titanium dioxide · Visible light photocatalytic activity · Photocatalyst

1 Introduction

Photocatalytic destruction of organic pollutants in the presence of TiO_2 appears as a viable decontamination process of widespread application. This is mainly due to its favorable properties like non-toxicity, chemical inertness, stability over a wide pH range under irradiation conditions [1–4] and its relatively favorable disposition of band edges. However, the anatase TiO_2 can be activated under UV light of wavelength under 387 nm irradiation due to its lager band-gap of 3.2 eV. Therefore, the optical response of TiO_2 shifting into the visible-light region will enhance its photocatalytic activity since solar spectrum usually containing about 4% UV light. Many techniques have been examined to achieve this purpose, such as, dye sensitized [5, 6], transition metals doping [7, 8], noble metal deposition [9, 10].However, these techniques suffer from thermal instability and an increasing number of carrier recombination centers. Moreover, the dye sensitized TiO_2 will suffer oxidative attack from reactive oxygen species(ROS) which may destroy photocatalyst and hinder the capacity of absorb visible light. Recently, C, N, S, F, B anion-doped TiO_2 photocatalysts that show a relatively high level of activity under visible-light irradiation have been reported [1, 11–15]. The theory of how non-metal element doping increase the photocatalytic activity of TiO_2 in visible light has still been controversial. Some researchers hold that the doping element(X) has formed Ti–X bond [12, 16]. However, Burda et al. [17] observed N 1 s core level at 401.3 eV from the detailed XPS investigations of nano N–TiO_2 and suggested that there is N–Ti–O bond formation due to nitrogen doping and no oxidized nitrogen is present. Despite of all the controversy, non-metal element doping is a novel method to prepare TiO_2 photocatalyst with improved visible light photocatalytic activity. In order to improve the photocatalytic activity, co-doped titania with double non-metal elements has attracted more attention. N–S co-doped TiO_2 powders were synthesized for decompositions of both acetaldehyde and trichloroethelene

X. Li · R. Xiong · G. Wei (✉)
College of Materials Science and Engineering,
Beijing University of Chemical Technology,
Beisanhuan Donglu 15, 100029 Beijing, China
e-mail: weigangmail@263.net

X. Li
e-mail: sandkingczar@gmail.com

R. Xiong
e-mail: xiongrongchun@263.net

[18]. Yu et al. [19] had developed N–S co-doped TiO_2 by hydrolysis of $Ti(SO_4)_2$ in a NH_3 H_2O solution. They exhibited that the photocatalytic activity of the as-prepared TiO_2 powders calcined at a temperature range of 400–700 C are obviously higher than that of P25. However, the most methods are high-temperature processes [20], using expensive preparation instruments [12].

Sol–gel method is very simple and does not require any special equipment. TiO_2 prepared by this method have well-crystalline phase and small crystalline size, which benefit to thermal stability and photocatalytic activity. In this work, a single anatase phase of S–N co-doped TiO_2 photocatalyst had been prepared by a sol–gel method using $Ti(OC_4H_9)_4$ as Ti source, thiourea as nitrogen and sulfur source. This work may provide new insights into the preparation of highly visible-light photoactive TiO_2 powders. The photocatalytic activity was evaluated by degradation of penicillin solution since penicillin was the main pollutant of antibiotic wastewater.

2 Experimental

2.1 Preparation

All chemicals used in this study were reagent-grade without further purification. The pure TiO_2 powders (called TiO_2-0) were synthesized by hydrolysis of $Ti(OC_4H_9)_4$ in a distilled water. The details are as follows: A mixture of 5 mL distilled H_2O and 10 mL ethanol (AR) was added drop wise at room temperature to a mixture of 5 mL $Ti(OC_4H_9)_4$(AR) and 15 mL ethanol. After stirring for 2 hours, a light-yellow transparent solution was formed. After it had gelatinized for 24 h at room temperature, a TiO_2 gel with white color was formed. The gel was heated at a rate of 2 C/min and calcined at 450 C for 2 h in a program control oven to get the powdered samples. To prepare co-doped TiO_2 samples, the as-prepared mixture of distilled water and ethanol was mixed with thiourea and was added to the mixer of $Ti(OC_4H_9)_4$ and ethanol. The obtained gel was heated at a rate of 2 C/min and calcined at certain temperature for 2 h in a program control oven to get the powdered samples. The heat temperature is 450, 550, 650 C, and the obtained powders were labeled as TiO_2-1, TiO_2-2, TiO_2-3. The color of the calcined powder sample changes and is from pale yellow to white with increasing the temperature. The reference samples used are P25, the Degussa P25 TiO_2.

2.2 Characterization

The X-ray diffraction (XRD) patterns obtained on a X-ray diffractometer (Type XRD-6000X Shimadzu,Japan) using Cu Kα irradiation at a scan rate of 5 $2\theta s^{-1}$ were used to determine the identity of any phase present and their crystalline size. The accelerating voltage and the applied current were 40 kV and 15 mA, respectively. The average crystallite sizes of TiO_2 were determined according to the Scherrer equation. X-ray photoelectron spectroscopy (XPS) measurements were done with a VG ESCALAB 250 X with an Mg Kα source. The shift of binging energy due to relative surface charging was corrected using the C1 s level at 284.8 eV as an internal standard. UV–Vis absorbance spectra of TiO_2 powders were obtained for the dry-pressed disk samples using a UV–Vis spectrophototmeter (UV 2550, Shimadzu, Japan). $BaSO_4$ was used as a reflectance standard in a UV–Vis absorbance experiment.

2.3 Measurement of Photocatalytic Activity

The photocatalytic activity of the as-prepared TiO_2 powders was evaluated by measuring the decomposition of penicillin aqueous solution with initial COD of 300. The UV photocatalytic reaction was carried out in a glass immersion photochemical reactor charged with 200 mL penicillin aqueous solution; the used amount of catalyst was 0.1 g. The vis-light photocatalytic experiments were carried out in the same reactor using a 40 W fluorescent lamp (main wavelength at 465 nm) as visible-light source. Prior to photocatalytic experiment, the catalysts were settled in suspension for 30 min in the dark for the adsorption equilibrium. The COD of penicillin solution were quantified by a COD meter (HACH,US). Three replicates were performed for each of samples.

The photocatalytic activity of the catalysts can be quantitatively evaluated by comparing the degradation rate ($\eta\%$). Degradation rate ($\eta\%$) was calculated according to the following equation:

$$\eta = \frac{COD_0 - COD_t}{COD_0} \times 100\% \quad (1)$$

Where COD_0 and COD_t represent the initial equilibrium COD and reaction COD of penicillin aqueous solution, respectively.

3 Results and Discussion

3.1 Phase Structure

Figure 1 gives the XRD patterns of S–N co-doped TiO_2 powers calcined at different temperature. All the samples showed a anatase phase. The Scherrer crystallite sizes were determined using the formula $t = 0.9\lambda/\beta\cos\theta$ where λ is the wavelength characteristic of the Cu Kα radiation, β is the full width at half maximum and θ is the angle at which the 100 intensity perk appears. The lattic parameters(a and c)

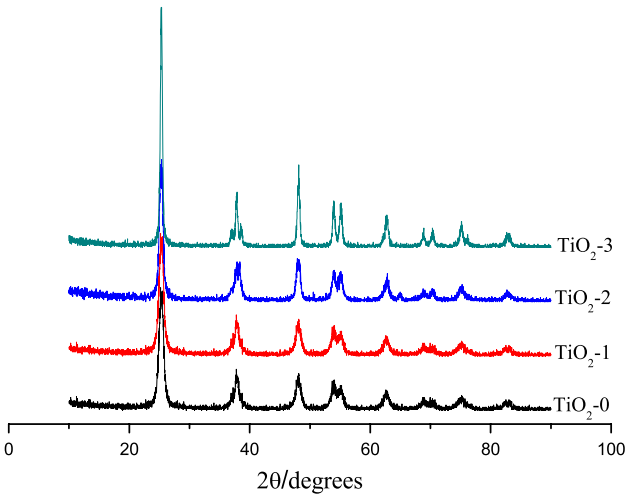

Fig. 1 XRD patterns of as prepared TiO_2 powders

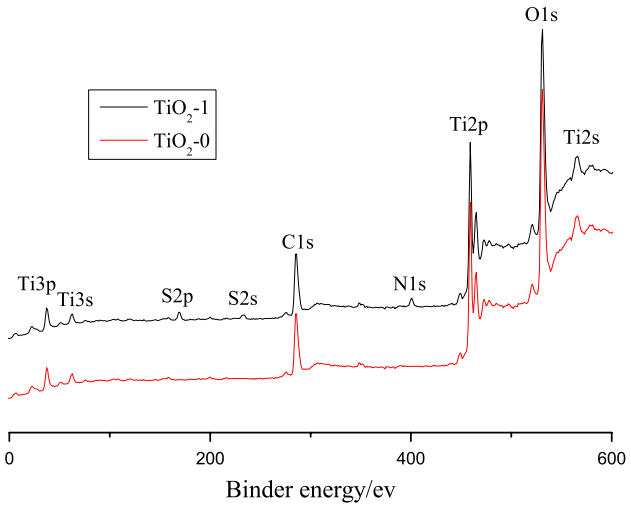

Fig. 2 XPS survey spectra of the un-doped sample TiO_2-0 and S–N co-doped sample TiO_2-1

Table 1 Characteristics of samples

Sample	Crystallite size(nm)	Unit cell parameter		
		a(Å)	*c*(Å)	*v*(nm^3)
[a]TiO_2		3.783	9.497	0.1359
TiO_2-1	10.7	3.789	9.517	0.1366
TiO_2-2	13.8	3.787	9.507	0.1363
TiO_2-3	21.3	3.785	9.504	0.1361

[a] JCPDS no.86-1157

were determined using the formula $1/d^2 = h^2/a^2 + k^2/b^2 + l^2/c^2$, where *h*,*k*,*l* are the miller indices and d is the interplanar distance. The Scherrer crystallite sizes, lattice parameter are as given in Table 1.

From Table 1 it can be obtained that the particle size increased with the calcination temperature increased. The increased particle size favorers the recombination of carriers since photoinduced electrons and holes cannot easily reach the surface within their lifetimes limiting the formation of surface ROS [21]. The unit cell parameters of TiO_2-3 remained almost unchanged, indicating that S,N is not weaved into the crystal structure of the sample. However, the unit cell parameters of TiO_2-1 are affected greatly, which means that S and N co-doped into the lattice of TiO_2.

3.2 XPS Analysis

Figure 2 shows the XPS survey spectra of the un-doped sample A and S–N co-doped sample B powders. It can be seen that the un-doped sample A only contains Ti, O and C elements, with sharp photoelectron peaks appearing at binding energies of 458 (Ti 2p), 531 (O 1 s) and 285 eV (C 1 s). The atomic ratio of Ti to O of the sample A is about 2, in good agreement with the nominal atomic composition of TiO_2. The carbon peak is attributed to the residual carbon from the sample and adventitious hydrocarbon from XPS instrument itself. On the contrary, the co-doped sample B not only contains Ti, O and C, but also a small amount of N and S atoms(binding energies at 401 and 169 eV, respectively), which probably come from the precursor $CS(NH_2)_2$ during the calcinations.

Figure 3 shows the corresponding high-resolution XPS spectra of N 1 s region taken from the sample TiO_2-1. It can be seen that the curve of N 1 s region of the sample

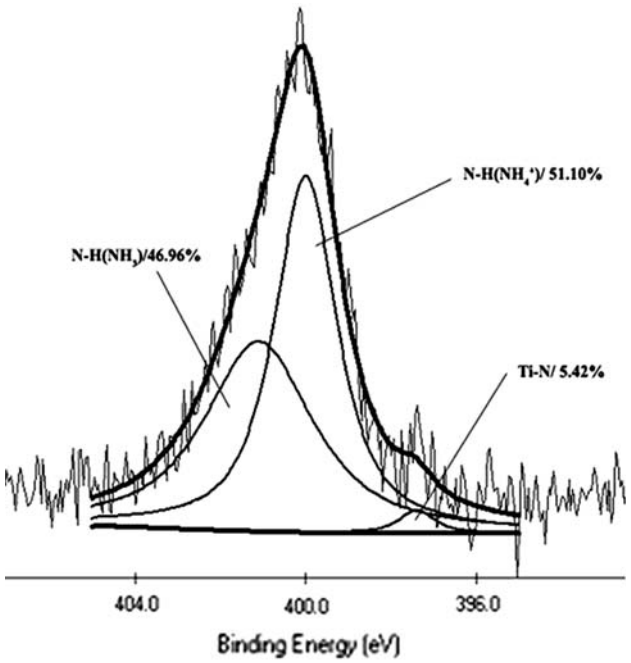

Fig. 3 High-resolution XPS spectra for the N 1s region of the sample TiO_2-1

TiO_2-1 can be deconvoluted into three peaks. A small one is attributed to the Ti–N(binging energy at 397.4 eV) [22, 23], which is probably formed by a nucleophilic substitution reaction between $CS(NH_2)_2$ and TiO_2 during calcinations. The other two peaks at about 400.0 and 401.1 eV are probably assigned to some NH_3 and NH_4^+ adsorbed on the surface of TiO_2 respectively [11, 19]. The state of doped nitrogen in the TiO_2 lattice and the mechanism of band gap reduction has still been in arguing. Asahi et al. [12] stated the N 1 s core lever at binding energy between 396 and 397 eV which is explained in the oxidation of TiN. Additional N 1 s peaks on nitrogen doped TiO_2 were observed at 400 and 402 eV are attributed to chemisorbed N_2 or adsorbed organic impurities [12, 16].However, Satish [24] et al. observed a N 1 s core level at 398.2 from the XPS investigations of nitrogen doped TiO_2 and suggested that there in N–Ti–O bond formation due to nitrogen doping and no oxidized nitrogen is present. Diwald [25] observed an N 1 s peak at binding energy of 399.6 eV which is effective in reducing the photon energy for photochemistry. It is to be noted that the preparation procedure adopted was different in the above cases and this could lead to the different observations in XPS.

Figure 4 shows the high-resolution XPS spectrum of the S 2p region of TiO_2-1. It could be observed that S 2p peak of TiO_2-1 contains two peaks at binding energy of 169.0 and 164.8 eV. The peak at 169 eV can be deconvoluted two peaks at 168.5 and 169.6 eV respectively. Both peaks can be attributed to the S(+VI). The S(+VI) may be assigned to SO_4^{2-} ions adsorbed on the surface of TiO_2 powders. The peak at 164.8 eV corresponds to the Ti–S bond due to the fact that S atom replace O atom in TiO_2 lattice [26]. It can be reasonable to deduce that if the S^{2-} ions replace the O^{2-} ions in the lattice of TiO_2, a lattice distort may be created due to a large ionic radius difference between S^{2-}(1.7Å) and O^{2-}(1.22Å) [27]. XRD results further confirm the above deduction. The cell parameters *a* and *c* (calculated according to XRD result) of the S–N co-doped sample TiO_2-1 were 3.789 and 9.517 Å, respectively, which were slightly bigger than those of pure anatase TiO_2(JPCDS Card 86-1157, *a* = 3.783 Å, *c* = 9.474 Å, space group:I41/amd). According to the above XPS results, no Ti–S, Ti–N peak was observed in the un-doped sample TiO_2-0, further implying that S,N elements were in situ doped into TiO_2 powders during calcinations.

3.3 UV–Vis Diffuse Reflectance Spectra

Figure 5 shows the UV–Vis absorption spectra of the P25 and S–N co-doped TiO_2 powders. A significant increase in the adsorption at wavelengths shorter than 400 nm can be assigned to the intrinsic band-gap adsorption of TiO_2. The absorption spectra of the S–N co-doped TiO_2 samples show a stronger absorption in the visible light region and a red shift in the adsorption edge.

The red shift is ascribed to the fact that S–N co-doping can narrow the band-gap of the TiO_2 Further observation shows that the absorbance decreases with increasing calcination temperature. At 650 C, the absorbance of S–N co-doped TiO_2 in the UV region is similar to that of P25 and the absorbance in the visible region is higher than that of P25. At 450 C, the absorbance of S–N co-doped TiO_2 is obviously higher than that of P25 in the whole UV–Vis light region and a red shift in the adsorption edge. This may be attributed the fact that calcination can induce S and N elements doped into the lattice of TiO_2, resulting in the narrowing of the band gap. However, it can be seen that the light absorption of S–N co-doped TiO_2 in the visible region

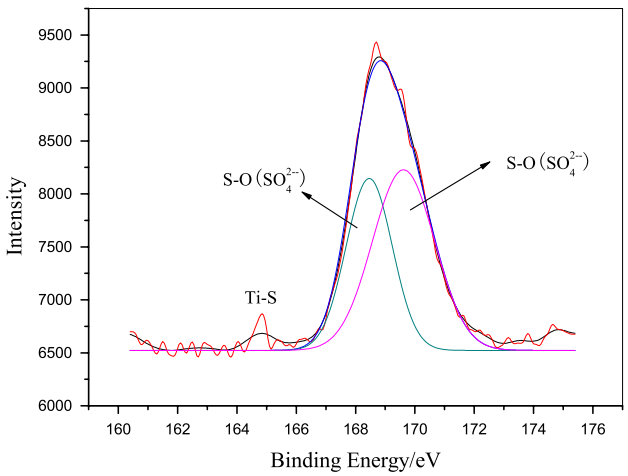

Fig. 4 High-resolution XPS spectrum of the S 2p region of the sample TiO_2-1

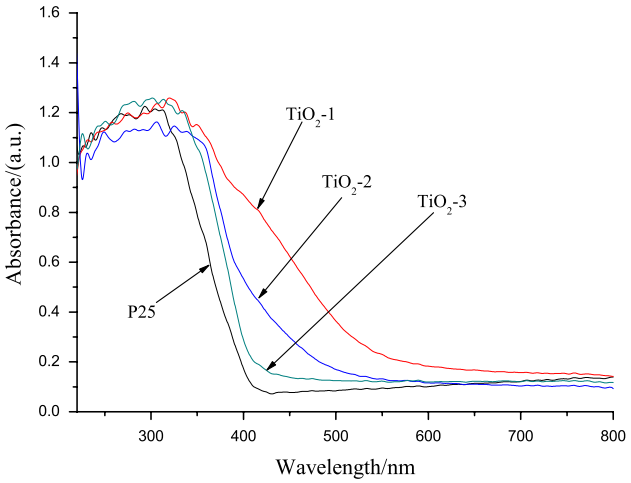

Fig. 5 UV–Vis absorption spectra of P25 and S–N co-doped TiO_2 powders

decrease very significantly as the calcination temperature increase. It could due to that high calcination temperature could enlarge the particle size which lead non-metal element atom hard into the TiO_2 lattice. It can be seen from Table 1 that the cell parameter of TiO_2-3 remained unchanged comparing to TiO_2-1, meanwhile, the particle size of TiO_2-3 is bigger than TiO_2-1. Previous reference [28] have report that it will be more easy for doping N element into TiO_2 when the particle size of TiO_2 is less than 10 nm It has also been observed in an earlier report [29] that an increase in the calcination temperature decreased the amount of heteroatom doping in TiO_2.

The absorption edge shifts to longer wavelengths for the S–N co-doped TiO_2 powders with decreasing calcinations temperature. This clearly indicates a decrease in the band-gap energy of TiO_2. The band gap of the samples can be determined by the equation [30].

$$Eg = 1239.8/\lambda \quad (2)$$

Where Eg is the band-gap(eV) and λ(nm) is the wavelength of the absorption edges in the spectrum. Thus, the indirect band-gap energy estimated from the absorption edges are about 2.16, 2.53 and 2.94 eV for the S–N co-doped TiO_2 samples TiO_2-1, TiO_2-2, TiO_2-3, respectively. The indirect band-gap energy of P25 is 3.0 eV. Therefore, it is no doubt the indirect band-gap energy of the as-prepared powders is much lower than that of anatase TiO_2 due to S–N codoping.

3.4 Photocatalytic Activity

The photocatalytic activity of the prepared TiO_2 powders was quantificationally evaluated by photocatalytic degradation of penicillin solution. The photocatalytic behavior of P25 was also measured as a reference to that of the as-prepared TiO_2 powders. However, the COD of penicillin solution does not change using various as-prepared TiO_2 powders under dark condition. Illumination in the absence of TiO_2 powders does not result in the photocatalytic reaction. Therefore, the presence of both illumination and TiO_2 powders is necessary for the efficient degradation. Figure 6 shows the degradation rate (η) of photocatalytic oxidation of penicillin solution under visible light of TiO_2-0 to TiO_2-3, and P25. It can be seen that the degradation rate of TiO_2-0 sample(pure TiO_2) has a very low visible light induced photocatalytic activity. This is due to the fact that the un-doped TiO_2 powders have the biggest indirect band-gap energy of about 3.2 eV. When a small amount of S and N atoms is doped into TiO_2 powders, the visible light induced photocatalytic activity of the prepared samples increases. At calcination temperature at 450 C, the photocatalytic activity of the co-doped sample TiO_2-1 powders reaches a maximum value, and its activity exceeds that of

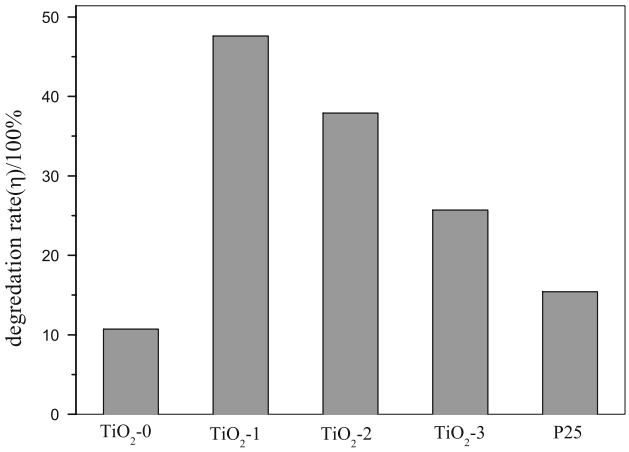

Fig. 6 Photocatalytic activity of as-prepared TiO_2 powders samples and P25 under visible light

P25 by a factor of three times. With further increasing the calcination temperature, the photocatalytic activity decreases. One possible explanation for this photocatalytic activity decay is that the substituted non-metal atoms in the doped TiO_2 lattice have been completely substituted by oxygen atoms with calcinations temperature rising. Therefore, we concluded that 450 C is the transition temperature, at which the doped TiO_2 photocatalyst could have suitable band gap by S–N codoping, resulting in the highest visible light activity.

Usually, the doping non-metal elements in TiO_2 play an important role in its visible-light photocatalytic activity. It can be seen from Fig. 5 that the S–N codoping results in an intense increase in absorption in the near UV and visible-light region and a red shift in the absorption edge of the S–N co-doped TiO_2 samples. This implies that the S–N co-doped TiO_2 can be activated by visible light and generated more photo-induced electrons and holes to participate the reaction. Hence, the band-gap narrowing of TiO_2 by S–N codoping results in enhanced photocatalytic activity of prepared TiO_2 powders. Hashimoto and co-workers [31, 32] provided an alternative explanation that a localized N 2p state formed above the valence band was the origin for the visible light activity of the nitrogen-doped TiO_2. Yu et al. [26] found that sulfur doping can indeed create intra-band gap state close to the conduction band edge, and thus induces visible-light absorption at the sub-band gap energy.

The decrease in the photocatalytic activity of the S–N codoped TiO_2 powders calcined at above 550 C is due to the following factors. The sintering and growth of TiO_2 crystallites will result decrease of surface area of the TiO_2 powders. Also with the increasing of particles size the recombination of charge will be improved which will affect the photocatalytic activity. Meanwhile, the growth of crystallites will cause loss of non-metal atoms in situ of TiO_2.

4 Conclusion

Highly photoactive S–N co-doped TiO_2 photocatalysts can be successfully prepared by a simple sol–gel method. This method can efficiently dope sulfur and nitrogen elements into the lattice of TiO_2. The S–N co-doped TiO_2 powders exhibit a stronger adsorption in the near UV and visible—light region and a red shift in the band-gap transition. The photocatalytic activities of as prepared S–N co-doped TiO_2 in visible-light region are about three times higher than that of Degussa P25. The highly photoactivities of the as-prepared TiO_2 is ascribed to a synergetic consequence of several beneficial effects such as the improvement in UV–Vis vacancies, red shift in adsorption edge. However, the photocatalytic activities decrease with the calcination temperature increases which can be attributed to the result that high calcination temperature lead larger particle size. Meanwhile, large particle size can cause loss of non-metal atoms in situ of TiO_2 lattice.

Acknowledgement This project was financially supported by National High-Tech Research and Development Program of China (Grant Number: 2007AA05Z409).

References

1. Fujishima A, Honda K (1972) Nature 238:37
2. Hoffmann MR, Martin ST, Choi W, Bahnemann DW (1995) Chem Rev 95:69
3. Hsien Y, Chang C, Chen Y, Cheng S (2001) Appl Catal B 31:241
4. Fujishima A, Rao Tata N, Donald AJ (2000) Photochem Photobio C 1:1
5. Watson DF, Marton A, Stux et al (2003) J Phys Chem B 107:10971
6. Clifford JN, Palomares E et al (2004) J Am Chem Soc 126:5670
7. Anpo M, Takeuchi M (2003) J Catal 216:505
8. Zhao W, Chen CC, Li XZ et al (2002) J Phys Chem B 106:5022
9. Subramanian V, Wolf EE, Kamat P (2004) J Am Chem Soc 126:4943
10. Jakob M, Levanon H, Kamat PV (2003) Nano Lett 3:353
11. Yu JC, Yu J, Ho W, Jiang Z, Zhang L (2002) Chem Mater 14:3808
12. Asahi R, Morikawa T, Ohwaki T, Aoki K, Taga Y (2001) Science 293:269
13. Umebayashi T, Yamaki T, Itoh H, Asai K (2002) Appl Phys Lett 81:454
14. Irie H, Watanabe Y, Hashimoto K (2003) Chem Lett 32:772
15. Chen DM, Yang D, Wang Q, Jiang ZY (2006) Chem Res 45:4110
16. Sano T, Negishi N, Koike K, Takeuchi K, Matsuzawa SJ (2004) Mater Chem 14:380
18. Gole JL, Stout JD, Burda C, Lou Y, Chen XJ (2004) Phys Chem B 108:1230
18. Liu HY, Gao L (2004) J Am Ceram Soc 87:1582
19. Yu JG, Zhou MH, Cheng B, Zhao XJ (2006) J Mol Catal A 246:176
20. Kosowska B, Mozia S, Morawski AW et al (2005) Sol Energy Mater Sol Cells 88:269
21. Almquist CB, Biswas P (2002) J Catal 212:145
22. Nakamura R, Tanaka T, Nakato Y (2004) J Phys Chem B 108:10617
23. Sakthivel S, Janczarek M, Kisch H (2004) J Phys Chem B 108:19384
24. Sathish M, Viswanathan B, Viswanath RP, Gopinath CS (2005) Chem Mater 17:6349
25. Diwald O, Thompson TL, Goralski EG, Walck SD, Yates JT (2004) J Phys Chem B 108:6004
26. Yu JC, Ho WK, Yu JG, Yip H, Wong PK, Zhao JC (2005) Environ Sci Technol 39:1175
27. Bacsa R, Kiwi J, Ohno T, Albers P, Nadtochenko V (2005) J Phys Chem B 109:5994
28. Burda C, Chen XB, Gole JL et al (2003) Nano Lett 3:1049
29. Ohno T, Mitsui T, Matsumura M (2003) Chem Lett 32:364
30. Oregan B, Gratzel M (1991) Nature 353:737
31. H Irie, S Washizuka, N Yoshino, K Hashimoto (2003) Chem Commun 1298
32. Irie H, Watanabe Y, Hashimoto K (2003) J Phys Chem B 107:5483